

Photoinitiated Electron Collection at a Metal in a Rhodium-Centered Mixed-Metal Supramolecular Complex

Mark Elvington and Karen J. Brewer*

Department of Chemistry, Virginia Polytechnic Institute and State University, Blacksburg, Virginia 24060-0212

Received February 15, 2006

A mixed-metal supramolecular complex $[\{(bpy)_2Ru(dpp)\}_2RhCl_2]^{5+}$ has been studied and shown to undergo photoinitiated electron collection at the metal center. Reported herein is an analysis of the photochemical properties of this complex, illustrating the ability of this complex to photoreduce by two electrons by converting Rh^{III} to Rh^I and with the trimetallic assembly remaining intact. Emission-quenching experiments demonstrate efficient quenching of the $Ru \rightarrow dpp$ charge-transfer state by the Rh center and the electron-donor dimethylaniline.

The conversion of light energy into chemical energy is of great interest, with particular focus on the development of efficient solar energy conversion schemes. The metal-to-ligand charge-transfer (MLCT) excited states of ruthenium polyazine complexes have found widespread use in this arena.^{1–3} Multielectron photocatalysis is a key component of schemes to convert light energy into fuels. Both solar water splitting and light-driven carbon dioxide reduction invoke multielectron reactions. Much work has focused on the development of complex supramolecular assemblies for light harvesting and directional charge separation.^{4–6} Very few homogeneous systems have been studied that use light to perform multielectron reactions or collect reducing equivalents.^{7–10} We report herein a Rh-centered supramo-

lecular complex that undergoes photoinitiated electron collection at the Rh center.

Photoinitiated electron collection is a process where light energy is used to collect reducing equivalents. This multi-electron photochemistry has been of interest in harvesting light energy as a means to produce multielectron-reduced substrates or fuels. A system for photoinitiated electron collection must efficiently absorb light, undergo efficient successive and/or multiple electron transfer(s), and be stable in the multielectron-reduced form, making functional photoinitiated electron collectors (PECs) elusive.

The first functioning photoinitiated EC was reported by Brewer, employing π systems of polyazine bridging ligands (BLs) to collect electrons, $[\{(bpy)_2Ru(BL)\}_2IrCl_2]^{5+}$ ($bpy = 2,2'$ -bipyridine).⁷ This complex photochemically collects multiple electrons on the π systems of BLs bound to a central metal.

MacDonnell, Campagna, and co-workers reported two interesting bimetallic Ru complexes that collect two or four electrons photochemically.⁸ These systems function by optical excitation into a phen-type orbital on the BL followed by transfer to a lower-lying secondary π^* acceptor orbital. Photolysis of $(phen)_2Ru(tatpq)Ru(phen)_2^{4+}$ leads to the four-electron-reduced complex $tatpq = phenanthroline$ –pyrazine–quinone–pyrazine–phenanthroline.⁸

Bocarsly and co-workers devised promising Pt^{IV} -centered trimetallic complexes $[\{(NC)_5M^{II}(CN)\}_2Pt^{IV}(NH_3)_4]^{4-}$ ($M = Fe, Ru, \text{ or } Os$) that undergo photoinitiated electron transfer.¹⁰ In the case where $M = Fe$, absorption of one photon results in two-electron transfer to the central Pt^{IV} followed by fragmentation of the polymetallic complex into two Fe^{III} complexes and a reduced Pt^{II} monometallic complex.¹⁰

Nocera and co-workers designed interesting metal–metal-bonded systems that undergo photochemical multielectron chemistry.⁹ Photolysis of $(PPh)_3Rh^0$ – $Rh^0(MeN(PF_2)_2)_3(CO)$

- (1) (a) Campagna, S.; Serroni, S.; Puntoriero, F.; Di Pietro, C.; Ricevuto, V. In *Electron Transfer in Chemistry*; Balzani, V., Ed.; Wiley-VCH: New York, 2001; Vol. 5, p 168 and references cited therein. (b) Balzani, V.; Moggi, L.; Manfrin, M. F.; Bolletta, F.; Laurence, G. A. *Coord. Chem. Rev.* **1975**, *15*, 321.
- (2) Meyer, T. J. *Pure Appl. Chem.* **1986**, *58*, 1576.
- (3) Kalyanasundaram, K. *Coord. Chem. Rev.* **1982**, *46*, 159.
- (4) Balzani, V.; Moggi, L.; Scandola, F. In *Supramolecular Photochemistry*; Balzani, V., Ed.; NATO Advanced Study Institute Series 214; Reidel: Dordrecht, The Netherlands, 1987; p 1 and references cited therein.
- (5) Balzani, V.; Juris, A.; Venturi, M.; Campagna, S.; Serroni, S. *Chem. Rev.* **1996**, *96*, 759 and references cited therein.
- (6) Serroni, S.; Campagna, S.; Puntoriero, F.; Loiseau, F.; Ricevuto, V.; Passalacqua, R.; Galletta, M. C. *R. Chim.* **2003**, *6*, 883.
- (7) Molnar, S. M.; Nallas, G.; Bridgewater, J. S.; Brewer, K. J. *J. Am. Chem. Soc.* **1994**, *116*, 5206.
- (8) (a) Konduri, R.; Ye, H.; MacDonnell, F. M.; Serroni, S.; Campagna, S.; Rajeshwar, K. *Angew. Chem., Int. Ed.* **2002**, *41* (17), 3185. (b) Chiorboli, C.; Fracasso, S.; Scandola, F.; Campagna, S.; Serroni, S.; Konduri, R.; MacDonnell, F. M. *Chem. Commun.* **2003**, 1658. (c) Chiorboli, C.; Fracasso, S.; Ravaglia, M.; Scandola, F.; Campagna, S.; Wouters, K.; Konduri, R.; MacDonnell, F. *Inorg. Chem.* **2005**, *44* (23), 8368.

- (9) (a) Heyduk, A. F.; Nocera, D. G. *Science* **2001**, *293*, 1639. (b) Nocera, D.; Heyduk, A. *PCT Int. Appl.* **2003**, 157. (c) Gray, T.; Nocera, D. *Chem. Commun.* **2005**, *12*, 1540. (d) Esswein, A.; Veige, A.; Nocera, D. *J. Am. Chem. Soc.* **2005**, *127* (47), 16641.
- (10) (a) Chang, C. C.; Pfennig, B.; Bocarsly, A. B. *Coord. Chem. Rev.* **2000**, *208*, 33. (b) Watson, D. F.; Tan, H. S.; Schreiber, E.; Mordas, C. J.; Bocarsly, A. B. *J. Phys. Chem. A* **2004**, *108*, 3261. (c) Mordas, C.; Pfennig, B.; Schreiber, E.; Bocarsly, A. B. *Springer Ser. Chem. Phys.* **2003**, *71*, 453.

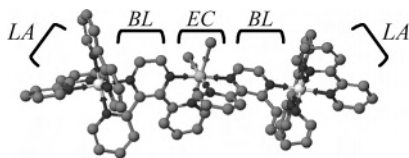


Figure 1. Mixed-metal supramolecular complex $[(\text{bpy})_2\text{Ru}(\text{dpp})_2\text{RhCl}_2]^{5+}$, a molecular device for photoinitiated electron collection [light absorber (LA), bridging ligand (BL), and electron collector (EC), bpy = 2,2'-bipyridine, and dpp = 2,3-bis-2-pyridylpyrazine].

results in photodissociation of CO and coordination of hydrohalic acid. Disproportionation produces H_2 and $(\text{PPh}_3)_3\text{Rh}^0\text{-Rh}^0(\text{MeN}(\text{PF}_2)_2)_3\text{X}_2$ (X = halogen). Adding a halogen atom trap leads to regeneration of the catalytically active species $(\text{PPh}_3)_3\text{Rh}^0\text{-Rh}^0(\text{MeN}(\text{PF}_2)_2)_3$.⁹

Herein we report photochemical properties of $[(\text{bpy})_2\text{Ru}(\text{dpp})_2\text{RhCl}_2](\text{PF}_6)_5$ [Figure 1; dpp = 2,3-bis-2-pyridylpyrazine]¹¹ coupling two Ru light absorber (LA) units, through polyazine BLs, to a central Rh EC core. This trimetallic complex undergoes unique, previously unreported photochemistry. Photoinitiated electron collection at Rh reduces Rh^{III} to Rh^{I} with the trimetallic assembly remaining intact.

Tris(polyazine)rhodium(III) complexes are known to serve as electron acceptors in intermolecular electron-transfer schemes utilizing $[\text{Ru}(\text{bpy})_3]^{2+}$ LAs.¹² Upon MLCT excitation of $[\text{Ru}(\text{bpy})_3]^{2+}$, bimolecular electron transfer to $[\text{Rh}(\text{bpy})_3]^{3+}$ yields $[\text{Rh}(\text{bpy})_3]^{2+}$, which disproportionates to $[\text{Rh}(\text{bpy})_2]^{+}$ and $[\text{Rh}(\text{bpy})_3]^{3+}$ or in the presence of a Pt catalyst generates H_2 .¹²

The trimetallic complex $[(\text{bpy})_2\text{Ru}(\text{dpp})_2\text{RhCl}_2](\text{PF}_6)_5$ displays light-absorbing properties dominated by the two Ru LA units and redox properties that illustrate the $\text{Rh}(d\sigma^*)$ nature of the lowest unoccupied molecular orbital (LUMO).¹¹ Electrochemically, this complex displays two reversible, overlapping $\text{Ru}^{\text{III/II}}$ couples at 1.63 V vs Ag/AgCl, indicating that the two Ru centers are largely electronically uncoupled (see the Supporting Information). Reductively, an irreversible $\text{Rh}^{\text{III/I}}$ couple at -0.37 V and two reversible $\text{dpp}^{0/-}$ couples at -0.76 and -1.00 V are observed. This illustrates the $\text{Ru}(d\pi)$ nature of the highest occupied molecular orbital and $\text{Rh}(d\sigma^*)$ nature of the LUMO. The electronic absorption spectroscopy shows bpy- and dpp-based $\pi \rightarrow \pi^*$ transitions in the UV and $\text{Ru} \rightarrow \text{bpy}$ and $\text{Ru} \rightarrow \text{dpp}$ CT transitions in the visible.¹¹ The lowest energy band observed in the electronic absorption spectrum is a $\text{Ru} \rightarrow \text{dpp}$ CT transition at 520 nm.

Emission spectroscopy was used to investigate the photophysical properties of $[(\text{bpy})_2\text{Ru}(\text{dpp})_2\text{RhCl}_2]^{5+}$. Emission from the dpp-based $^3\text{MLCT}$ state at 760 nm is quenched by intramolecular electron transfer to the Rh, thereby populating the lower-lying metal-to-metal charge-transfer ($^3\text{MMCT}$) state. Compared to the model bimetallic system without Rh $[(\text{bpy})_2\text{Ru}(\text{dpp})\text{Ru}(\text{bpy})_2]^{4+}$,¹³ $\lambda_{\text{max}}^{\text{em}} = 744$ nm, $\Phi^{\text{em}} = 1.38 \times 10^{-3}$ [measured vs $\text{Os}(\text{bpy})_3^{2+}$],¹⁴

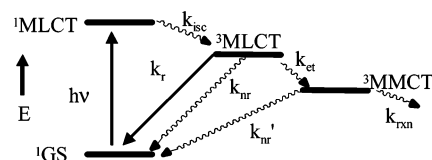


Figure 2. State diagram for $[(\text{bpy})_2\text{Ru}(\text{dpp})_2\text{RhCl}_2]^{5+}$, a molecular device for photoinitiated electron collection (bpy = 2,2'-bipyridine and dpp = 2,3-bis-2-pyridylpyrazine).

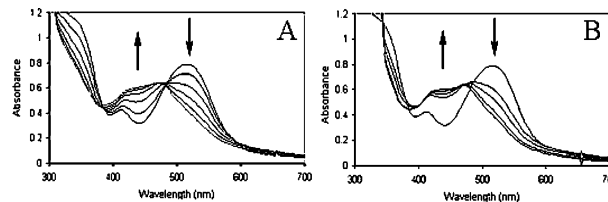


Figure 3. Electronic absorption spectra for the conversion of $[(\text{bpy})_2\text{Ru}(\text{dpp})_2\text{Rh}^{\text{III}}\text{Cl}_2]^{5+}$ to the two-electron-reduced form $[(\text{bpy})_2\text{Ru}(\text{dpp})_2\text{Rh}^{\text{I}}]^{5+}$ electrochemically (A) and photochemically (B) (bpy = 2,2'-bipyridine and dpp = 2,3-bis-2-pyridylpyrazine). Electrochemically (A), the complex is reduced at -0.40 V vs Ag/AgCl in deoxygenated 0.1 M $\text{Bu}_4\text{PF}_6/\text{CH}_3\text{CN}$ in an H cell. (B) The complex is photolyzed at 520 ± 10 nm in deoxygenated CH_3CN with 0.29 M DMA.

the title trimetallic complex exhibits 95% quenching of the $^3\text{MLCT}$ emission ($\Phi^{\text{em}} = 7.3 \times 10^{-5}$) and a concurrent reduction in the excited-state lifetime in a deoxygenated room-temperature CH_3CN solution. Owing to the similar energy and $\text{Ru} \rightarrow \mu\text{-dpp}$ CT nature of both excited states, we estimate that k_r and k_{nr} are equivalent. This predicts efficient intramolecular electron transfer for $[(\text{bpy})_2\text{Ru}(\text{dpp})_2\text{RhCl}_2]^{5+}$, $k_{\text{et}} = 1.2 \times 10^8$ s⁻¹, populating the $\text{Ru} \rightarrow \text{Rh}$ $^3\text{MMCT}$ state (Figure 2).

The title complex $[(\text{bpy})_2\text{Ru}(\text{dpp})_2\text{Rh}^{\text{III}}\text{Cl}_2]^{5+}$ undergoes photoreduction in the presence of an electron donor, dimethylaniline (DMA), to produce the two-electron-reduced form $[(\text{bpy})_2\text{Ru}(\text{dpp})_2\text{Rh}^{\text{I}}]^{5+}$, thereby undergoing photoinitiated electron collection at the metal center. The electrochemical reduction by two electrons of $[(\text{bpy})_2\text{Ru}(\text{dpp})_2\text{Rh}^{\text{III}}\text{Cl}_2](\text{PF}_6)_5$ at -0.40 V leads to the formation of a Rh^{I} complex, $[(\text{bpy})_2\text{Ru}(\text{dpp})_2\text{Rh}^{\text{I}}](\text{PF}_6)_5$, via loss of two chlorides, analogous to $[\text{Rh}(\text{bpy})_2\text{Cl}_2]^+$ and $[\text{Rh}(\text{dpp})_2\text{Cl}_2]^+$.^{14,15} DeArmond observes that two-electron reduction of $[\text{Rh}(\text{bpy})_2\text{Cl}_2]^+$ produces an irreversible oxidation due to free chloride and two $\text{bpy}^{0/-}$ couples. Similarly, reduction of $[(\text{bpy})_2\text{Ru}(\text{dpp})_2\text{Rh}^{\text{III}}\text{Cl}_2]^{5+}$ by two electrons results in an irreversible chloride oxidation and two low-potential $\mu\text{-dpp}^{0/-}$ reductions at -0.76 and -1.00 V vs Ag/AgCl. The spectroscopic changes associated with the reduction of $[(\text{bpy})_2\text{Ru}(\text{dpp})_2\text{RhCl}_2]^{5+}$ are illustrated in Figure 3A. The $\text{Ru} \rightarrow \text{dpp}$ CT band shifts to higher energy for the Rh^{I} complex as a result of the decreased electron-withdrawing and increased electron-donating ability of Rh^{I} vs Rh^{III} , destabilizing the dpp π^* acceptor orbitals. This shift is mirrored by a movement to higher energy of the dpp-based $\pi \rightarrow \pi^*$ band. The $\text{Ru} \rightarrow \text{bpy}$ CT band at 420 nm is relatively unaffected by Rh reduction. Photolysis of $[(\text{bpy})_2\text{Ru}(\text{dpp})_2\text{Rh}^{\text{III}}\text{Cl}_2]^{5+}$ in the presence of a sacrificial

(11) Holder, A. A.; Swavey, S.; Brewer, K. J. *Inorg. Chem.* **2004**, *43*, 303.

(12) (a) Brown, G. M.; Chan, S. F.; Creutz, C.; Schwarz, H. A.; Sutin, N. *J. Am. Chem. Soc.* **1979**, *101*, 7638. (b) Creutz, C.; Keller, A. D.; Sutin, N.; Zipp, A. P. *J. Am. Chem. Soc.* **1982**, *104*, 3618.

(13) Fuchs, Y.; Lofters, S.; Dieter, T.; Shi, W.; Morgan, S.; Streckas, T. C.; Gafney, H. D.; Baker, A. D. *J. Am. Chem. Soc.* **1987**, *109*, 2691.

(14) Caspar, J. V.; Kober, E. M.; Sullivan, B. P.; Meyer, T. J. *J. Am. Chem. Soc.* **1982**, *104*, 630.

(15) Rasmussen, S. C.; Richter, M. M.; Yi, E.; Place, H.; Brewer, K. J. *Inorg. Chem.* **1990**, *29*, 3926.

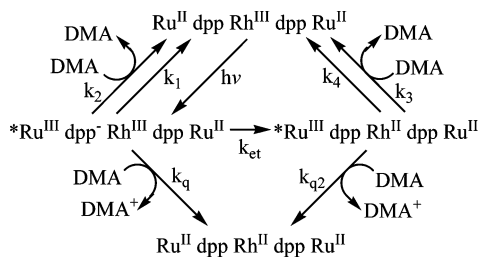


Figure 4. Proposed mechanism for photoinitiated electron transfer. bpy, Cl, and charges are omitted for clarity. $\text{Ru}^{\text{II}}\text{dppRh}^{\text{III}}\text{dppRu}^{\text{II}} = \{[(\text{bpy})_2\text{Ru}(\text{dpp})_2\text{RhCl}_2]^{5+}$ (bpy = 2,2'-bipyridine and dpp = 2,3-bis-2-pyridylpyrazine). DMA = dimethylaniline. k_1 and k_4 are the unimolecular decay pathways from the $^3\text{MLCT}$ and $^3\text{MMCT}$ states, respectively, whereas k_2 and k_3 are the bimolecular deactivation rates from the same states. k_{et} is the rate of electron transfer to generate the $^3\text{MMCT}$ state. k_q and k_{q2} are the rates of reductive quenching by DMA to generate the Rh^{II} complex from the $^3\text{MLCT}$ and $^3\text{MMCT}$ states, respectively.

electron donor, DMA, leads to the production of the same $\{[(\text{bpy})_2\text{Ru}(\text{dpp})_2\text{Rh}^{\text{I}}]^{5+}$ species (Figure 3B). The changes in the high-energy visible region of the spectrum are obscured in the photochemical experiment because of intense absorbance by DMA. The spectroscopic changes associated with the photochemical reduction (Figure 3B) are identical with those seen in the electrochemical reduction (Figure 3A). This study illustrates the ability of $\{[(\text{bpy})_2\text{Ru}(\text{dpp})_2\text{RhCl}_2](\text{PF}_6)_5$ to undergo photoinitiated electron collection at the Rh center.

A kinetic investigation has been undertaken to probe photoreduction of $\{[(\text{bpy})_2\text{Ru}(\text{dpp})_2\text{RhCl}_2]^{5+}$ in more detail. The generation of the two-electron-reduced form of our trimetallic complex, $\{[(\text{bpy})_2\text{Ru}(\text{dpp})_2\text{Rh}^{\text{I}}]^{5+}$, appears to occur through production of the Rh^{II} form, consistent with the electrochemical properties of $[\text{Rh}(\text{bpy})_2\text{Cl}_2]^+$ and $[\text{Rh}(\text{dpp})_2\text{Cl}_2]^+$.^{15,16} Our kinetic analysis focuses on the initial photochemical steps leading to the first-electron reduction of the trimetallic complex (Figure 4).

An emission-quenching analysis by the sacrificial donor DMA provides insight into the reactivity of the $^3\text{MLCT}$ state (Figures 2 and 4). The interaction between $[\text{Ru}(\text{bpy})_3]^{2+}$ and DMA has been studied previously.¹⁷ For $[\text{Ru}(\text{bpy})_3]^{2+}$, the $^3\text{MLCT}$ is quenched by DMA at a rate of $7.1 \times 10^7 \text{ M}^{-1} \text{ s}^{-1}$. For $^*\text{Ru}(\text{bpy})_3^{2+}$, the excited-state reduction potential is 0.77 V and the oxidation potential for DMA is 0.81 V (vs SCE).¹⁶ The excited-state reduction potential for $\{[(\text{bpy})_2\text{Ru}(\text{dpp})_2\text{RhCl}_2]^{5+}$ is 0.90 V, increasing the driving force for reductive quenching of the $\text{Ru} \rightarrow \text{dpp}$ CT state. The $^3\text{MLCT}$ state of the trimetallic complex undergoes competitive electron transfer to Rh to generate the $^3\text{MMCT}$ state. This gives rise to a complicated mechanism.

Emission from the $^3\text{MLCT}$ state of $\{[(\text{bpy})_2\text{Ru}(\text{dpp})_2\text{RhCl}_2]^{5+}$ is quenched efficiently by DMA (Figure 5A). Using the mechanism in Figure 4, $\Phi_0^{\text{em}}/\Phi^{\text{em}} = 1 + (k_q + k_2)/(k_1 + k_{\text{et}}[\text{DMA}])$. The slope of the Stern–Volmer plot (using $k_1 = k_r + k_{\text{nr}} = 1.2 \times 10^8 \text{ s}^{-1}$) yields $k_q + k_2 = 2 \times 10^{10} \text{ M}^{-1} \text{ s}^{-1}$, consistent with efficient $^3\text{MLCT}$ emission quenching. Back electron transfer for amine quenching of ruthenium

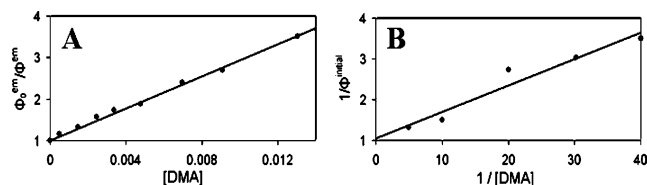


Figure 5. Stern–Volmer plots for (A) emission quenching of $\{[(\text{bpy})_2\text{Ru}(\text{dpp})_2\text{RhCl}_2]^{5+}$ by DMA and (B) product formation of the one-electron-photoreduced Rh^{II} product (bpy = 2,2'-bipyridine and dpp = 2,3-bis-2-pyridylpyrazine).

polyazine systems is often efficient, reducing the net product formation. In the case of $^*\text{Ru}(\text{bpy})_3^{2+}$ quenched by DMA, $k_q = 7.1 \times 10^7 \text{ M}^{-1} \text{ s}^{-1}$ and $k_b = 4.1 \times 10^9 \text{ M}^{-1} \text{ s}^{-1}$.¹⁷

To investigate the formation of the photoreduced Rh^{II} product in more detail, a Stern–Volmer analysis of product formation was undertaken (Figure 5B). At early photolysis times, the formation of Rh^{II} dominates and would display $\text{Ru} \rightarrow \text{dpp}$ CT transitions intermediate between the Rh^{III} and Rh^{I} forms. At high $[\text{DMA}]$, Φ_{initial} approaches unity. Product formation can occur from the $^3\text{MLCT}$ or $^3\text{MMCT}$ state or a combination of both. Kinetically, if product formation comes from the $^3\text{MLCT}$ state, $1/\Phi = (k_1 + k_{\text{et}})/(k_q[\text{DMA}]) + (k_q + k_2)/k_q$. Conversely, if product formation comes from the $^3\text{MMCT}$ state, $1/\Phi = (1/\Phi_{\text{MMCT}})(k_4/(k_{q2}[\text{DMA}]) + (k_{q2} + k_3)/k_q$. Both pathways predict the linear plot of $1/\Phi$ vs $1/[\text{DMA}]$ observed in Figure 5B, which yields a slope of 0.065 and a y intercept of 1.05. If the Rh^{II} product results from the $^3\text{MLCT}$ state, k_q would be $1.9 \times 10^9 \text{ M}^{-1} \text{ s}^{-1}$. The higher k_q for quenching of the trimetallic complex by DMA relative to $[\text{Ru}(\text{bpy})_3]^{2+}$ would be consistent with the increased driving force for electron transfer. If the Rh^{II} product results from quenching of the $^3\text{MMCT}$ state, k_4/k_{q2} is 0.062 and the value of k_{q2} would depend on the lifetime of the $^3\text{MMCT}$ state. Related trichelated systems show rapid back electron transfer ($7.1 \times 10^9 \text{ s}^{-1}$),¹⁸ which would require a very rapid k_{q2} . The above emission-quenching analysis and this product formation analysis suggest that both the $^3\text{MLCT}$ and $^3\text{MMCT}$ states may lead to photoreduced products.

The ability to reduce a metal center by multiple electrons within a supramolecular architecture that remains intact is unique and promising. The photoreduced product $\{[(\text{bpy})_2\text{Ru}(\text{dpp})_2\text{Rh}^{\text{I}}]^{5+}$ is coordinatively unsaturated, available to interact with substrates. Interestingly, this reduced complex still possesses an intense MLCT band that might be exploited for further photochemical reduction. Studies exploring the photochemical properties of this complex in more detail are underway.

Acknowledgment is made to the donors of the American Chemical Society Petroleum Research Fund for support of this work.

Supporting Information Available: Cyclic voltammogram of $\{[(\text{bpy})_2\text{Ru}(\text{dpp})_2\text{RhCl}_2](\text{PF}_6)_5$. This material is available free of charge via the Internet at <http://pubs.acs.org>.

(16) Kew, G.; DeArmond, M. K.; Hanck, K. J. *J. Phys. Chem.* **1974**, *78*, 727.

(17) (a) Anderson, C. P.; Salmon, D. J.; Meyer, T. J.; Young, R. C. *J. Am. Chem. Soc.* **1977**, *99* (6), 1980. (b) Haga, M.; Dodsworth, E.; Eryavec, G.; Seymour, P.; Lever, B. *Inorg. Chem.* **1985**, *24*, 1901.

(18) Indelli, M. T.; Bignozzi, C. A.; Harriman, A.; Schoonover, J. R.; Scandola, F. *J. Am. Chem. Soc.* **1994**, *116*, 3775.